Investigating Haptic Feedback in Vision-Deficient Millirobot Telemanipulation

Naveed D. Riaziat, *Student Member, IEEE*, Onder Erin, *Member, IEEE*, Axel Krieger, *Senior Member, IEEE*, Jeremy D. Brown, *Member, IEEE*

***Abstract*—The evolution of magnetically actuated millirobots gives rise to unique teleoperation challenges due to their non-traditional kinematic and dynamic architectures, as well as their frequent use of suboptimal imaging modalities. Recent investigations into haptic interfaces for millirobots have shown promise but lack the clinically motivated task scenarios necessary to justify future development. In this work, we investigate the utility of haptic feedback on bilateral teleoperation of a magnetically actuated millirobot in visually deficient conditions. We conducted an N=23 user study in an aneurysm coiling inspired procedure, which required participants to navigate the robot through a maze in near total darkness to manipulate beads to a target under simulated fluoroscopy. We hypothesized that users will be better able to complete the telemanipulation task with haptic feedback while reducing excess forces on their surroundings compared to the no feedback conditions. Our results showed an over 40% improvement in participants' bead scoring, a nearly 10% reduction in mean force, and 13% reduction in maximum force with haptic feedback, as well as significant improvements in other metrics. Results highlight that benefits of haptic feedback are retained when haptic feedback is removed. These findings suggest that haptic feedback has the potential to significantly improve millirobot telemanipulation and control in traditionally vision deficient tasks.**

***Index Terms*—Haptics and Haptic Interfaces, Telerobotics and Teleoperation, Medical Robots and Systems**

I. INTRODUCTION

ROBOTIC surgery, which has often relied on rigid serial-link manipulator (SLM) architectures, is beginning to see a paradigm shift towards compliant and untethered robots in both the research and commercial spaces. Research into soft-surgical systems has resulted in pneumatically actuated grippers, tendon-driven endoscopes, and other novel compliant architectures (see [2] for a review). In the commercial space, Intuitive's Ion system is a continuum robot capable of navigating the lung's airways trans-orally [3]. Similarly, J&J's Monarch bronchoscopy and urology continuum robot and Siemens' Corpath endovascular continuum robot both demonstrate the versatility of this architecture [4], [5]. Similarly, research into miniature untethered magnetic systems has led to the development of systems for future clinical applications [6], [7]. This research has also yielded some commercial teleoperated magnetic manipulation systems, such as Stereotaxis's endovascular surgery system and Levita Magnetics's abdominal surgery system, and many ongoing studies are in the preclinical and clinical validation stages [8], [9]. These recent advances promise to further reduce surgical invasiveness and improve outcomes by targeting anatomies traditionally inaccessible to rigid robots. To accomplish this, continuum and tetherless robots must consider the additional challenge of telenavigation.

For tetherless magnetic robots in particular, the same architectural novelties that imbue benefits over their rigid SLM counterparts contribute to some notable teleoperation challenges. First, milliscale magnetic devices have necessitated visualization either by external modalities (MRI, CT, etc.) or on-board, low resolution, monocular vision due to space

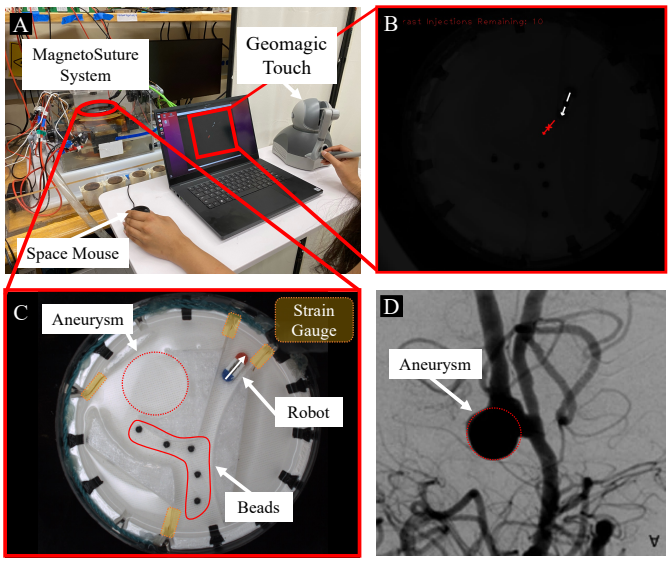

Fig. 1: (a) A user controlling the MagnetoSuture system. (b) A capture of the typical visual condition shown to the user without contrast injections. Users can improve their vision with a 0.5 second contrast injection up to 10 times per trial. (c) The robot task space with force sensing strain gauges highlighted in yellow. The robot is labeled with a white arrow in the top right. Beads are shown in their approximate starting locations. (d) Medical image of cerebral aneurysm showing the inspiration of maze layout [1].

Manuscript received: November 29, 2023; Revised February 23, 2024; Accepted April 3, 2024. This paper was recommended for publication by Editor Jessica Burgner-Kahrs upon evaluation of the Associate Editor and Reviewers' comments. This work was supported by NIH Award R01EB033354 and NSF CAREER grant 2144348.

N. D. Riaziat, A. Krieger, and J. D. Brown are with the Department of Mechanical Engineering, Johns Hopkins University, 3400 North Charles Street, Baltimore, Maryland, USA nriaziat@jhu.edu

O. Erin was previously with the Department of Mechanical Engineering, Johns Hopkins University, 3400 North Charles Street, Baltimore, Maryland, USA. He is now with Johnson and Johnson, 5490 Great America Parkway, Santa Clara, California, USA

Digital Object Identifier (DOI): see top of this page.

constraints. Compared to SLM robots, clinicians lose high quality imaging with miniaturized untethered systems and replace it with relatively noisy, high-latency visual feedback. In sub-optimal visual feedback and in small scales, estimating tool-tissue interactions becomes more challenging and may lead to increased risk of surgical complications like damage to delicate tissue due to excessive force [10], [11]. Second, tetherless magnetic robots feature kinematically complicated control schemes which make one-to-one correspondence with a telemanipulator challenging. While systems like Intuitive's da Vinci create a clear mapping between the interface and the tool, the non-mechanical kinematic chains of tetherless robots often obfuscate these mappings. Perhaps as a result of these visualization and manipulation challenges, researchers have relied most heavily on demonstrating autonomous capabilities of such systems (e.g. [12], [13], [14]).

Given the task performance [15], [16], [17], [18] and skill development [19], [20], [21], [22] benefits of kinesthetic (i.e. force) and tactile feedback, haptic interfaces have the potential to overcome the challenges in tetherless robot teleoperation. Unfortunately, the research on bilateral (force-reflecting) teleoperation in magnetic robots has been nascent. Of the few bilateral teleoperation studies that have been published, many show promise. Lee et al. for example, developed a method that generates a virtual 3D haptic environment reconstructed from 2D images in the control of magnetic millirobots [23]. Similarly, Ciuti et al. tested a force-feedback manipulator to control their magnetic capsule robot, mapping the position of their tethered robot to a 6-DoF haptic manipulator, and found that a serial-link haptic device performed optimally for teleoperated capsule endoscopy [24]. Finally, Pacchierotti et al. demonstrated in two separate systems that rendered force feedback with respect to robot trajectory error and desired position improved task performance even relative to vibrotactile feedback in a magnetic rigid robot and a soft-gripper robot [25], [26].

While these previous investigations of haptic force-feedback interfaces have demonstrated force feedback's potential utility in magnetic millirobot manipulation, three key gaps in knowledge remain. First, these studies all featured high-resolution visual feedback, which is significantly better than intraoperative imaging in terms of fidelity, temporal resolution, and the presence of noise and artifacts. Second, these studies utilized simple tasks that tested either trajectory following or pick-and-place performance, but not both concurrently as is common in clinical procedures. Finally, no study has reported the effect of haptic feedback on environmental forces (i.e. forces from surrounding structures like tissue) – a critical factor in delicate surgical interventions. Instead, haptic feedback has been provided to an a priori trajectory. Given the task dependent nature of haptic feedback utility [27], it is crucial to: a) understand the utility of haptic interfaces on performance metrics such as force reduction, and b) determine useful haptic feedback strategies in more clinically motivated scenarios involving degraded visual feedback and complex tasks involving navigation and manipulation.

In this manuscript, we evaluate a control interface that provides force feedback for a magnetic millirobot in a clinically inspired task with limited vision. We develop a EMI-hardened force sensor which, to the best of our knowledge, is a first for magnetic robotics. In order to understand how haptic feedback impacts teleoperation performance in limited vision, we asked participants to navigate a maze and manipulate objects using a robot with and without force feedback. While performing the task, participants are provided with limited visual feedback mimicking fluoroscopic imaging. Our findings provide early insight towards optimal control interfaces for magnetic robots that may impact future teleoperation interfaces and strategies, perhaps in eventual surgical applications. Key contributions of this paper are: (a) a real-time, model-based digital-twin haptic feedback strategy, (b) open-source design files for our force sensor, and (c) a rigorous user study investigating the utility of haptic feedback for millirobot telemanipulation in visually deficient conditions.

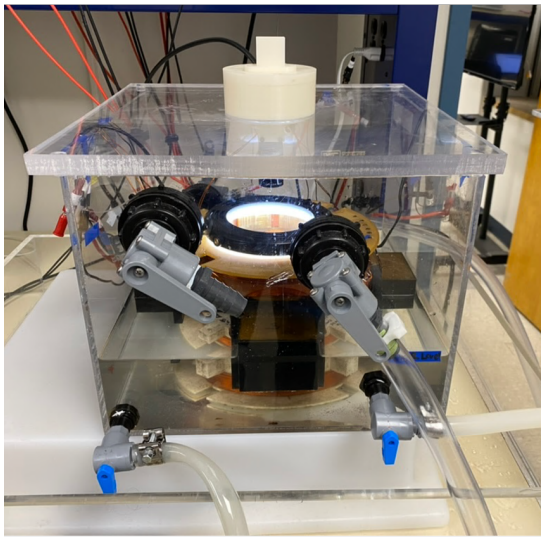

Fig. 2: The MagnetoSuture system is housed in an acrylic cube with pumped water coolant partially immersing the electromagnetic coils. The workspace, fixed in the center of the four coils, is imaged with the overhead camera.

II. Methods

The experimental methods are summarized into the following sections: a) the Teleoperation Test Platform, which is the source of the magnetic fields that control the millirobot, b) the Force Sensing Maze, which is a compliant, EMI hardened system used to collect environmental interaction forces for analysis purposes, and c) the Haptic Feedback system which leverages real time registration and physics simulation in the AMBF digital twin to generate haptic feedback.

A. Teleoperation Test Platform

The MagnetoSuture system, shown in Figure 2, is designed with four electromagnetic coils arranged orthogonally in a plane. Each coil has its current supply controlled via a DC motor driver and an Arduino. The system is powered with a 3.6 kW power supply. More detail about the system can be

found in [13]. We selected this system as our testbed for non-SLM magnetic teleoperation due to its large, planar workspace and high force output capability.

The MagnetoSuture was originally teleoperated with a gamepad style position-velocity mapping. For this study, we integrated a Geomagic Touch (3D Systems) for a position-position mapped control architecture with haptic feedback, as this haptic interface choice is consistent with prior work [24], [28]. In this implementation, the Geomagic Touch's 3D input is transformed onto the planar workspace. A SpaceMouse (3Dconnexion) is used for orientation control via a angle-to-velocity mapping without haptic feedback. Within the MagnetoSuture's workspace, a magnetic robot operates in vegetable glycerin (1.49 Pa − s). A FLIR Blackfly S USB3 camera images the robot and computes its pose using colored markers on the robot.

The MagnetoSuture applies forces and torques by controlling coil currents. A reference position is read from the Geomagic Touch (see Fig. 1a) and force is set with a proportional-derivative (PD) controller. Command position and velocity are estimated via a Kalman filter. The command force is

$$\vec{F}(t) = k_p \vec{e}(t) + k_d \dot{\vec{e}}(t), \tag{1}$$

where k_p and k_d are non-negative proportional and derivative gains, and $\vec{e}(t) = \vec{p}_d(t) - \vec{p}(t)$ is the error between the commanded robot position $\vec{p}_d$ and the actual robot position $\vec{p}$. Open loop heading control sets the command torque $\vec{T} = \alpha \hat{h}$. To exert the commanded forces and torques on the robot, the appropriate coil currents $I \coloneqq \left[i_1, i_2, i_3, i_4\right]^{\mathrm{T}}$ are found by computing $I = A^{\dagger}\left[\vec{T}, \vec{F}\right]^{\mathrm{T}}$, where $A^{\dagger} = (A^T A)^{-1} A^T$ is the pseudoinverse of

$$A = \begin{bmatrix} \vec{m} \times \tilde{B}(\vec{p}) \\ \vec{m} \cdot \frac{\partial \tilde{B}}{\partial \vec{p}} \end{bmatrix} \tag{2}$$

.

Here $\tilde{B}(\vec{p})$ is the unit-current magnetic field from a coil at relative location $\vec{p}$, $\frac{\partial \tilde{B}}{\partial \vec{p}}$ is the Jacobian matrix of $\tilde{B}(\vec{p})$, and $\vec{m}$ is the robot's magnetic moment vector. Finite element methods (FEM), as first introduced by Erin et al. [13], are used to model the fields offline. During the online robot control, these results are interpolated from a lookup table to compute $A^{\dagger}$.

B. Force Sensing Maze

Prior evaluations of magnetic robot telemanipulation have neglected results regarding environmental interaction force, perhaps due to the challenge of the high electromagnetic interference (EMI) in the environment. Environmental interaction forces are a critical outcome considering the importance of delicate tissue handling for optimal clinical outcomes. Thus, we developed a 3D-printed maze with compliant features (see Fig. 1C), inspired by soft tissue in human vasculature. To capture environmental interaction forces, we integrated a strain gauge-based force measurement system that is designed to withstand EMI. This combination of compliant maze and EMI-hardened force measurement system enables an analysis of environmental forces.

We utilized back-to-back EMI-cancelling strain gauge pairs[1] to reduce the signal bias from EMI. The resistive changes from the maze's walls are amplified 128x via a quarter Wheatstone bridge and converted it to an 18-bit digital signal via our open source circuit board[2]. Our EMI-hardening achieved a 10 dB improvement in signal-to-noise ratio compared to traditional strain gauge amplification.

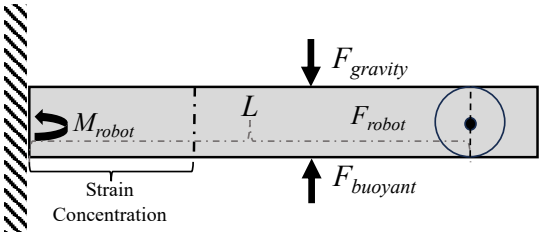

Fig. 3: A cantilevered beam from the maze is shown from the side. The thin base concentrates strain generated by the robot over the strain gauge.

We employed a cantilevered beam model to establish a mapping between measured strains and applied moments, as shown in Fig. 3. This model allows for real time moment measurement during the task. We approximate the loading condition as a simple point load F causing a small displacement at a distance L from the base of a cantilevered beam (Dirichlet boundary condition) with section modulus S and Young's modulus E. The strain is therefor $\varepsilon = FL/SE$.

Likewise, the governing equations for a quarter Wheatstone bridge are:

$$V_{bridge} = V_{exc}\left(\frac{R+\Delta R}{2R+\Delta R} - 0.5\right),\ \Delta R = R \cdot GF \cdot \varepsilon, \tag{3}$$

where GF is the gauge factor, R and ΔR are the nominal and change in resistance of a leg of the bridge, V_{bridge} is the voltage output, and V_{exc} is the excitation voltage.

Therefore, we compute the force on the wall as a function of the bridge voltage and robot location:

$$F(V_{bridge}, L) = \frac{-4Ebh^2 V_{bridge}}{6L(2GF * V_{bridge} - GF * V_{exc})}, \tag{4}$$

where F is the measured force, b is the wall's cross-sectional width, and h is the wall's cross-sectional height.

The walls of the maze were 3D-printed of Ultimaker nylon for its compliance (Ultimaker B.V, Utrecht, Netherlands). To calibrate our force estimation, we applied moments from 0.09 to 0.49 mN-m at 0.05 mN-m increments and one point at 1 mN-m on a wall fixtured vertically. The response was linear ($r^2 = 0.98$) for this range, with mean deviation of 10%. We expect this trend to stay linear under similar moments, as confirmed from our experimental results in Section III. Through FEM analysis, we predicted an typical strain of 10 mε and a peak voltage output of 10 mV.

The maze task is designed with four walls, each supported at one end with strain concentration at the base. The buoyant force of the glycerin allows the wall to float with minimal friction. A strain gauge is bonded with cyanoacrylate glue

[1]Tokyo Measuring Instruments Laboratory Co., Ltd, Japan, QMFLA-5-350-11-1LJAY-F

[2]https://github.com/nriaziat/EMI-Hardened-Force-Sensor-PCB

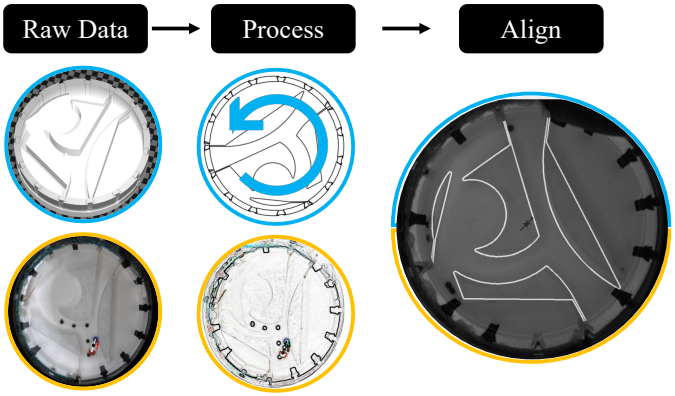

Fig. 4: The AMBF model is registered to the camera image by minimizing R from Equation 5. The final result shows the haptic collision boundaries aligned to the camera frame.

and sealed with conformal coating. The wall's linear mapping between voltage and strain is used to determine the instantaneously applied force. OpenCV records the origin for each wall and computes the robot's relative position. We compute the moment from the strain using our FEM results and deduce the applied force at 20 Hz.

C. Haptic Feedback

We developed a haptic feedback approach based in the Asynchronous Multi-Body Framework (AMBF) [29], which allows for kilohertz force-feedback based on physics simulation of a registered simulated digital twin of the environment. We chose this approach as opposed to the common Hooke's law force approach given the overall complexity of our task and findings against its efficacy in pilot investigations. In the AMBF digital twin approach, a collision mesh of the workspace was generated with a 2048 convex polygon decomposition using the V-HACD library [30]. Interaction of the digital twin with the user's pointer generate appropriate haptic response without showing any penetration. The mesh is aligned to the camera view via a transformation $T_{mc} \in SE(2)$ and scaling factor $s \in \mathbb{R}$. T_{mc} composes of a 2D translation $\vec{t}_{mc} \in \mathbb{R}^2$ and rotation $\theta \in \mathbb{R}$. The scaling factor is determined by the ratio of the pixel radius to the mesh radius in meters, $s = \frac{r_m}{r_c}$. The vector from the circle center in both reference frames define $\vec{t}_{mc} = \vec{p}_m - s\vec{p}_c$. Finally, a slice of the STL file $I'_a = sT_{mc} \cdot I_a - \text{mean}(I_a)$ is compared to the gradient of the camera frame $I'_c = \nabla I_c - \text{mean}(I_c)$ via their cross-correlation R and the resulting value is minimized across rotations, i.e., $\theta = \underset{\theta \in \mathbb{R}}{\text{argmin}} R(\theta)$,

$$R = -\frac{\sum_{x',y'} I'_c(x+x',y+y') I'_a(x',y')}{\sqrt{\sum_{x',y'} I'_c(x+x',y+y')^2 \sum_{x',y'} I'_a(x',y')^2)}}. \quad (5)$$

The minimizing transformation sT_{mc} is displayed to the experimenter visually for verification then passed to AMBF to register the mesh and camera frames (see Fig. 4). This method is inspired from the image template-matching problem.

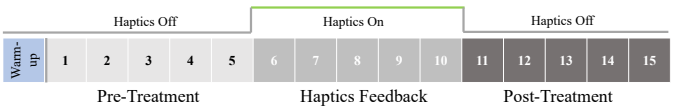

Fig. 5: Participants completed 15 trials in three 5-trial blocks: pre-treatment, haptic feedback, and post-treatment.

D. Computation

Software was written in C++ and Python 3.8. and runs on an Ubuntu 20.04 laptop with an Intel i7 CPU at a control loop rate of 60 Hz (limited by the camera's capture rate). The package coordinates between the coil controllers, camera, force sensor, input devices, and AMBF. FEM results are used to find unit-current field strength and gradients and determine appropriate coil currents. Inter-component communication is arbitrated through ROS 1 Noetic.

III. User Study

A. Experimental Task

Our experimental task requires: a) navigation of complex anatomy, b) manipulation of material within a small target workspace, and c) minimal forces. Our phantom maze is loosely inspired by anatomy of a neurovascular aneurysm, mimicking the tight confines, continuous curves, abrupt junctions, and compliant walls. The user utilizes the robot in the MagnetoSuture system to manipulate beads to the target. Fluoroscopic imaging is commonly used in aneurysm interventions alongside iodine-based contrast agents injections. However, frequent contrast injection increases the risk of complications [31]. Participants conducted the experiment with 5 Hz visual feedback through a low-contrast image. Up to ten times per 2-minute trial, the participant could use buttons on the control interface to improve image contrast for 0.5 seconds, for a total of 5 seconds per trial of 120 seconds. Users could always see both their commanded pose as well as the robot's current pose (see Figure 6). Though in clinical applications contrast injections may last much longer, the comparative simplicity and shorter timescale of our task necessitated a shorter contrast injection duration.

B. Participants and Study Design

Twenty-three participants (Mean age: 24.7±3.1; 7 women, 16 men; 22 right-handed, 1 ambidextrous) were recruited for this study from the general population at Johns Hopkins University. No participants had clinical experience, nor prior experience using the MagnetoSuture system. All participants provided written informed consent according to a protocol approved by the Johns Hopkins University Homewood Institutional Review Board (Study# HIRB00011569). Participants were compensated at a rate of $10/hour.

After providing informed consent, each participant completed a demographics survey. Once complete, the investigator would help adjust the height of the interfaces and the chair to participants' desired comfort level. After a brief demonstration of the interfaces by the investigator, the participants were

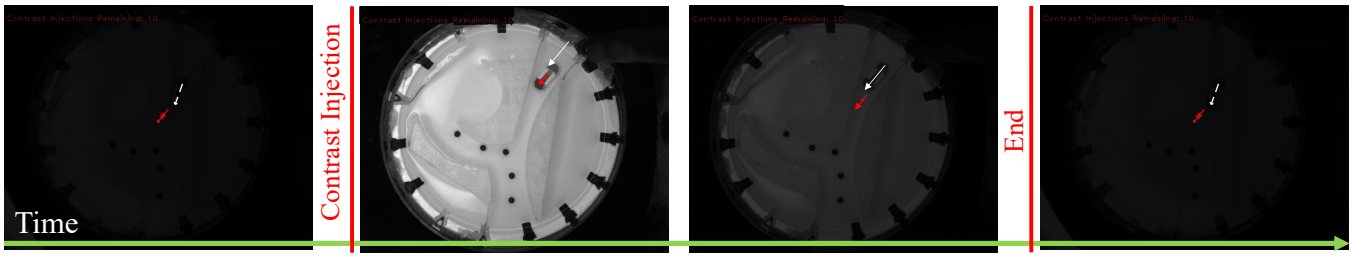

Fig. 6: Time series showing the user's vision before, during, and after a 0.5 second contrast injection. When the user clicks the button for a contrast injection, the contrast will instantly improve but quickly decay back to the prior condition.

TABLE I: Metrics employed in the user study.

Metric	Description
Beads Scored [BS]	# of beads scored
Wall Force [WF]	RMS environmental force [N]
Path Length [PL]	Robot trajectory length [m]
Log. Dimensionless Jerk [DJ]	Motion smoothness (related to skill)

allowed 2 minutes of supervised practice to control the robot with no specific aim. At this time, if the participant has any questions about the control interface or task, they could ask the investigator. After donning noise-cancelling headphones, the first block of five trials would begin. Between each trial, the participants would be given a minimum of 2 minutes rest (more if requested) while the experiment was reset. After each block, a longer break was given to allow for completion of a NASA Task Load Index (TLX) survey. The experiment would continue in this fashion until all three blocks were completed.

Each participant completed 15 consecutive trials of the experimental tasks broken into blocks of five trials. In the first block, denoted as "Pre-Treatment", participants did not receive haptic feedback. In the second block, denoted as "Haptic Feedback", kinesthetic haptic feedback was provided (as described in Section II-C). Finally in the third block, denoted as "Post-Treatment", haptic feedback was turned off again (see Fig. 5). Each task consisted of navigating the magnetic robot to the location of the small ceramic beads and then using the robot to push the beads into the region of interest (ROI). Participants were instructed to move as many beads into the ROI as possible in two minutes, while minimizing contact with the walls of the environment.

C. Metrics and Analyses

The metrics in Table I were used to analyze participants' performance in each trial of the task:

- *Beads Scored* (*BS*): the number of beads scored.
- *Wall Force* (*WF*): the root mean squared force applied to the walls.
- *Path Length* (*PL*): the distance traveled by the robot.
- *Logarithmic Dimensionless Jerk* (*DJ*): skill metric measured via the third derivative (smoothness) of the user's motion [32], [33].

Participants' qualitative assessment of the workload was evaluated using the validated NASA TLX survey [34] that was administered after each testing block. The survey asked participants to rate their mental demand, physical demand, temporal demand, performance, effort, and frustrations on a 5-point Likert scale with 1="Low' and 5="High'.

Linear mixed models (LMMs) were used to analyze the effect of learning and haptics on the metrics described above. LMMs are a generalized form of ANOVAs ("Analysis of variance") that fit data (e.g., metrics) to fixed variables (e.g., treatment condition) without normality assumptions, and accommodate data with repeated observations (multiple trials) and correlations across variables [35]. Therefore, one LMM can be used to analyze the entire dataset akin to separately using a repeated measures ANOVA and an ANCOVA ("Analysis of Covariance"), while also allowing for the analysis of non-continuous metrics like Beads Scored and TLX. LMM 1: $y \sim trial \cdot condition + (1|participant)$ included trial as a co-variate to test if task repetitions changed performance (natural learning). LMM 2: $y \sim condition + (1|participant)$ analyzed the effect of condition independently. Visual inspection of the residuals verified independence, homogeneity, and normality of errors. 95% confidence intervals and p-values were computed using a Wald t-distribution. Post-hoc pairwise comparisons in slopes were computed using Tukey's multiple contrasts of means. The Holm method was used to correct for familywise error rates.

Due to a system error, force data was not collected for three participants and thus three additional participants were recruited. The following statistical analyses were performed on the remaining 20 data sets for force related metrics, and the total 23 participants for all other metrics.

IV. Results

Detailed discussion of these results is found in Section V. Omitted comparisons were not statistically significant.

1) Beads Scored: BS in the haptic feedback condition was significantly higher than in the pre-treatment condition by 0.42 (29.2%, $p < 0.01$), and that the *BS* in the post-treatment condition was significantly higher than in the pre-treatment condition by 0.64 (44.6%, $p < 0.001$) (Figure 7A). Increased *BS* may indicate that users learned more effective control and retained this efficacy without haptics.

2) Wall Force: WF for the haptic feedback condition was significantly lower than in the post-treatment condition by 21 mN ($p = 0.045$) (Figure 7B). Maximum wall force showed

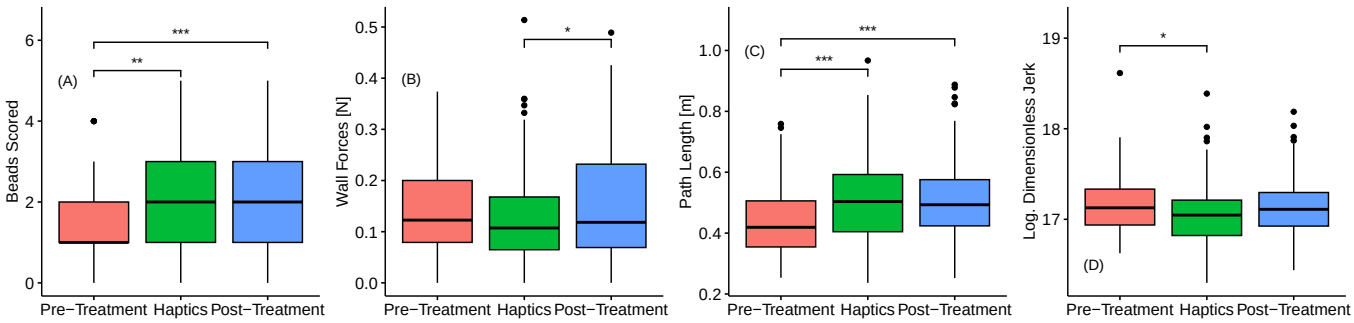

Fig. 7: Plots showing a) Beads Scored (*BS*), b) Wall Force (*WF*) c) Path Length (*PL*), and d) Logarithmic Dimensionless Jerk (*DJ*) per condition. *** $p < 0.001$, ** $p < 0.01$, * $p < 0.05$.

results approached significance ($p = 0.057$) with a 13% reduction during haptic feedback. RMS and maximum *WF* reductions indicate that haptic feedback helped users make more gentle interactions with their environment by relaying force information.

3) Path Length: *PL* in the haptic feedback condition was significantly greater than in the pre-treatment condition by 6.44 cm (14.5%, $p < 0.001$), and that *PL* in the post-treatment condition was significantly higher than in the pre-treatment condition by 6.83 cm (15.5%, $p < 0.001$) (Figure 7C). Increased *PL* aligns with the *BS* finding that users learned more effective control strategies by receiving haptic feedback.

4) Dimensionless Jerk: *DJ* with the haptic feedback condition was significantly lower than in the pre-treatment condition by 0.11 ($p = 0.014$) (Figure 7D). Reduced *DJ* during haptics indicates enhanced smoothness correlated with skillful operation.

5) TLX: Table II summarizes participant responses to the NASA TLX. The LMM showed that temporal demand was lower in post-treatment than pre-treatment ($p = 0.034$), performance was higher in post-treatment than pre-treatment or haptics ($p = 0.01$, $p = 0.1$), and effort is lower in post-treatment than in haptics ($p = 0.004$). We infer that users felt more comfortable with the task after the experiment completion and that haptics increased perceived effort since users may have felt impeded by forces on their hand. However, effect sizes are small in these comparisons so experienced differences were not substantial.

6) Natural Learning: The model with the learning covariate had a lower Akaike Information Criterion (AIC) and trial number was not a significant predictor ($p > 0.05$) of performance. We interpret that the condition effects were more substantial than natural learning during the trials.

V. Discussion

As small-scale robots increase in prevalence, it is critical to evaluate optimal teleoperation strategies for delicate navigation and manipulation tasks, especially under visually deficient conditions experienced in MRI or fluoroscopic visualization. In this study, we (a) developed a new, open-source force sensing platform for magnetic robots, (b) utilized AMBF to render real time registered haptic interactions, and (c) investigated whether haptic feedback positively impacts users' ability to perform a force-sensitive telenavigation and telemanipulation task, and whether those benefits are temporary or sustained after feedback is removed. Our force sensor was able to reduce EMI noise by 10 dB, allowing for the first environmental force measurement results in a magnetic robot teleoperation study to the best of our knowledge. The AMBF environment enabled 1 KHz haptic feedback by registering a 3D model to 2D images of the workspace. With these developments, participants manipulated beads to a target location by teleoperating a magnetically actuated robot with a haptic interface. Participants completed the task in three blocks and received haptic feedback in only the middle block. Overall, we found that haptic feedback had tangible benefits in a manner that was sustained once haptic feedback was removed.

1) Beads Scored: Haptic feedback and post-treatment both displayed higher Beads Scored *BS* than the pre-treatment. Haptic feedback may have allowed users to avoid excess forces created through wall interactions, reducing navigation time and increased scoring. This finding is consistent with literature in surgical training which has demonstrated improved task success with haptic feedback [16], [36]. Participants retained the visual-motor strategies learned with haptic feedback afterwards. This is consistent with prior work demonstrating skill retention in telerobotic surgery [37], and builds on prior results in magnetic robot manipulation [26] by demonstrating the utility of haptic feedback in a clinically motivated manipulation tasks. Our findings indicate that haptic feedback has lasting impact on user skill acquisition, whereas some studies have found the performance benefit to be temporary [21].

TABLE II: NASA TLX results (1 low, 5 high) for pre-treatment (P1), haptic feedback (H), and post-treatment (P2). Bold text indicates best value compared to value with †.

Question	P1	H	P2
Mental Demand	3.6±0.95	3.5±1.0	3.5±0.91
Physical Demand	2.6±1.1	2.9±1.2	2.6±1.1
Temporal Demand	4.0±1.1†	3.9±0.97	**3.6±1.2**
Performance	2.1±0.97†	2.3±0.95†	**2.8±1.0**
Effort	4.0±0.93	4.3±0.88†	**3.7±1.1**
Frustration	3.0±1.4	3.0±1.2	2.7±0.95

2) Wall Force: Haptic feedback decreased *WF* compared to post-treatment. This suggests that some skill can be maintained without haptic feedback while those requiring force estimation may not. In traditional telerobotic surgery, surgeons learn to compensate for the lack of haptic feedback through visual cues [10]. This skill, however, relies on HD stereoscopic visualization. In our task, clear visualization was only available through contrast injections. Thus, participants could not accurately estimate the forceful interactions without haptics. This result aligns with prior findings showing that haptic feedback leads to force reduction during telerobotic manipulation [16], [20], [36], [37].

3) Path Length: Our results also demonstrate that the haptic and post-treatment conditions resulted in significantly higher *PL* during the task. Haptic feedback may have taught participants to more effectively avoid obstacles and thus travel further. This is consistent with demonstrations of reduced task completion times with haptic feedback [38], [36].

Haptic feedback may imbue task-based knowledge that would not have been learned through repeated practice. This is supported by the fact that *PL* did not change significantly in the post-treatment condition.

4) Dimensionless Jerk: Users had lower *DJ* with haptic feedback, indicating higher skill. As such, providing haptic feedback to novice robot operators may be key in enhancing skill acquisition. This result is consistent with other findings which have shown improved motion smoothness with haptic feedback [39]. In future applications, one should note that haptic feedback may improve skill which was not retained in the post-treatment phase.

5) TLX: Users reported lower temporal demand in post-treatment than pre-treatment and lower effort in post-treatment than haptics, while performance was perceived to be best in post-treatment. This indicates that haptic feedback had additional cognitive load of interpreting the cues. However, users' perception of their performance and the temporal demand went down after haptics, suggesting that the condition contributed to their task learning. Interface designers should consider that haptic feedback may provide additional cognitive burden in some tasks, especially those that have no prior haptic intuition, but still provides a perceived training benefit to the user.

6) Natural Learning: Since trial number was not a statistically significant predictor of performance and worsened model fit, we interpret that performance changes are more attributed to treatment condition and not natural learning. This does not discount natural learning effects but instead suggests that the effect of treatment condition was significantly greater.

VI. Conclusions and Future Works

In this study, we evaluated the utility of a digital-twin based force-reflecting teleoperation control scheme for a tetherless magnetically actuated robot in a navigation and manipulation task with limited vision. To the best of our knowledge, this is the first study to directly measure and analyze forces in a magnetically-actuated robot. We found that haptic feedback lead to reduced robot-environment forces while also training task performance skills that were maintained after the feedback was removed. These findings are important to researchers developing advanced robotic systems that do not feature traditional serial link manipulator architectures as it suggests the benefit of including haptic feedback in the control interface, especially for early-stage skill development. In addition, this work demonstrates the importance of investigating robot-environment forces and establishes a method for measuring these forces in electromagnetically actuated robots. Finally, these preliminary findings provide support for continued investigation of *ex-vivo* tissue studies with clinicians in the future.

While these results provide robust insight into the utility of haptic feedback in surgical millirobots, there are a few limitations that should be addressed in future work. First, while the trend for better learning with haptic feedback is clear, the precise level of performance improvement is unknown. Future studies should compare a control group in which participants receive no haptic feedback to measure natural learning. Second, it is unclear to what extent, if any, the findings depend on the specific task utilized. Future investigations should test how well these benefits generalize, in particular one that utilizes real tissue or different maze permutations per trial. Third, in order to facilitate more direct comparison to prior work, identical haptic and visual conditions of this experiment may be provided to a-priori path following and manipulation tasks as in [26]. Finally, future research should investigate the potential utility of adding haptic feedback of bead interactions.

Acknowledgments

The authors would like to thank Jan Uli Bartels, Dr. Adnan Munawar, Sergio Machaca, and Alexandra J. Miller for their contributions to the study. This work was supported by the National Institutes of Health R01EB033354 and NSF CAREER grant 2144348. Any opinions, findings, and conclusions or recommendations expressed in this material are those of the author(s) and do not necessarily reflect the views of the National Institutes of Health or National Science Foundation.

References

[1] W. Sansom, "Studies compare best ways to treat wide-neck aneurysms," Feb. 2022. [Online]. Available: https://news.uthscsa.edu/studies-compare-best-ways-to-treat-wide-neck-aneurysms/

[2] P. E. Dupont, N. Simaan, H. Choset, and C. Rucker, "Continuum Robots for Medical Interventions," *Proceedings of the IEEE*, vol. 110, no. 7, pp. 847–870, Jul. 2022, conference Name: Proceedings of the IEEE. [Online]. Available: https://ieeexplore.ieee.org/abstract/document/9707607

[3] D. Fielding, F. Bashirzadeh, J. Son, M. Todman, A. Chin, L. Tan, K. Steinke, M. Windsor, and A. Sung, "First Human Use of a New Robotic-Assisted Fiber Optic Sensing Navigation System for Small Peripheral Pulmonary Nodules," *Respiration*, vol. 98, no. 2, pp. 142–150, Jul. 2019.

[4] C. F. Graetzel, A. Sheehy, and D. P. Noonan, "Robotic bronchoscopy drive mode of the Auris Monarch platform," in *2019 International Conference on Robotics and Automation (ICRA)*, May 2019, pp. 3895–3901.

[5] M. D. Christopher C. Smitson, M. D. Lawrence Ang, M. D. Ali Pourdjabbar, M. D. Ryan Reeves, M. D. Mitul Patel, and M. D. Ehtisham Mahmud, "Safety and Feasibility of a Novel, Second-Generation Robotic-Assisted System for Percutaneous Coronary Intervention: First-in-Human Report," *Journal of Invasive Cardiology*, vol. 30, no. 4, Jan. 2018.

[6] D. Son, H. Gilbert, and M. Sitti, "Magnetically Actuated Soft Capsule Endoscope for Fine-Needle Biopsy," *Soft Robotics*, vol. 7, no. 1, pp. 10–21, 2020.

[7] L. O. Mair, X. Liu, B. Dandamudi, K. Jain, S. Chowdhury, J. Weed, Y. Diaz-Mercado, I. N. Weinberg, and A. Krieger, "MagnetoSuture: Tetherless Manipulation of Suture Needles," *IEEE Transactions on Medical Robotics and Bionics*, vol. 2, no. 2, pp. 206–215, May 2020.

[8] I. N. Haskins, A. T. Strong, M. T. Allemang, K. P. Bencsath, J. H. Rodriguez, and M. D. Kroh, "Magnetic surgery: first U.S. experience with a novel device," *Surgical endoscopy*, vol. 32, no. 2, pp. 895–899, 2018.

[9] R. Luengas, J. Galindo, M. Castro, A. Marambio, G. Watkins, M. Rodriguez del Rey, C. Davanzo, D. Portenier, and A. D. Guerron, "First prospective clinical trial of reduced incision bariatric procedures using magnetic liver retraction," *Surgery for obesity and related diseases : official journal of the American Society for Bariatric Surgery*, vol. 17, no. 1, pp. 147–152, 2021.

[10] M. E. Hagen, J. J. Meehan, I. Inan, and P. Morel, "Visual clues act as a substitute for haptic feedback in robotic surgery," *Surgical Endoscopy*, vol. 22, no. 6, pp. 1505–1508, Jun. 2008.

[11] R. Nayyar and N. P. Gupta, "Critical appraisal of technical problems with robotic urological surgery," *BJU International*, vol. 105, no. 12, pp. 1710–1713, 2010, _eprint: https://onlinelibrary.wiley.com/doi/pdf/10.1111/j.1464-410X.2009.09039.x. [Online]. Available: https://onlinelibrary.wiley.com/doi/abs/10.1111/j.1464-410X.2009.09039.x

[12] Y. Dong, L. Wang, Z. Zhang, F. Ji, T. K. F. Chan, H. Yang, C. P. L. Chan, Z. Yang, Z. Chen, W. T. Chang, J. Y. K. Chan, J. J. Y. Sung, and L. Zhang, "Endoscope-assisted magnetic helical micromachine delivery for biofilm eradication in tympanostomy tube," *Science Advances*, vol. 8, no. 40, p. eabq8573, Oct. 2022, publisher: American Association for the Advancement of Science. [Online]. Available: https://www.science.org/doi/10.1126/sciadv.abq8573

[13] O. Erin, S. Raval, T. J. Schwehr, W. Pryor, Y. Barnoy, A. Bell, X. Liu, L. O. Mair, I. N. Weinberg, A. Krieger, and Y. Diaz-Mercado, "Enhanced Accuracy in Magnetic Actuation: Closed-Loop Control of a Magnetic Agent With Low-Error Numerical Magnetic Model Estimation," *IEEE Robotics and Automation Letters*, vol. 7, no. 4, pp. 9429–9436, Oct. 2022.

[14] Y. Dong, L. Wang, N. Xia, Z. Yang, C. Zhang, C. Pan, D. Jin, J. Zhang, C. Majidi, and L. Zhang, "Untethered small-scale magnetic soft robot with programmable magnetization and integrated multifunctional modules," *Science Advances*, vol. 8, no. 25, p. eabn8932, Jun. 2022, publisher: American Association for the Advancement of Science. [Online]. Available: https://www.science.org/doi/10.1126/sciadv.abn8932

[15] R. P. Khurshid, N. T. Fitter, E. A. Fedalei, and K. J. Kuchenbecker, "Effects of Grip-Force, Contact, and Acceleration Feedback on a Teleoperated Pick-and-Place Task," *IEEE Transactions on Haptics*, vol. 10, no. 1, pp. 40–53, Jan. 2017.

[16] A. Abiri, J. Pensa, A. Tao, J. Ma, Y.-Y. Juo, S. J. Askari, J. Bisley, J. Rosen, E. P. Dutson, and W. S. Grundfest, "Multi-Modal Haptic Feedback for Grip Force Reduction in Robotic Surgery," *Scientific Reports*, vol. 9, no. 1, p. 5016, Mar. 2019.

[17] A. Saracino, A. Deguet, F. Staderini, M. N. Boushaki, F. Cianchi, A. Menciassi, and E. Sinibaldi, "Haptic feedback in the da Vinci Research Kit (dVRK): A user study based on grasping, palpation, and incision tasks," *The International Journal of Medical Robotics and Computer Assisted Surgery*, vol. 15, no. 4, Aug. 2019.

[18] O. A. J. van der Meijden and M. P. Schijven, "The value of haptic feedback in conventional and robot-assisted minimal invasive surgery and virtual reality training: a current review," *Surgical Endoscopy*, vol. 23, no. 6, pp. 1180–1190, Jun. 2009. [Online]. Available: https://doi.org/10.1007/s00464-008-0298-x

[19] M. Zhou, S. Tse, A. Derevianko, D. B. Jones, S. D. Schwaitzberg, and C. G. L. Cao, "Effect of haptic feedback in laparoscopic surgery skill acquisition," *Surgical Endoscopy*, vol. 26, no. 4, pp. 1128–1134, Apr. 2012.

[20] C. R. Wottawa, J. R. Cohen, R. E. Fan, J. W. Bisley, M. O. Culjat, W. S. Grundfest, and E. P. Dutson, "The role of tactile feedback in grip force during laparoscopic training tasks," *Surgical Endoscopy*, vol. 27, no. 4, pp. 1111–1118, Apr. 2013.

[21] J. Lee and S. Choi, "Effects of haptic guidance and disturbance on motor learning: Potential advantage of haptic disturbance," in *2010 IEEE Haptics Symposium*, Mar. 2010, pp. 335–342, iSSN: 2324-7355. [Online]. Available: https://ieeexplore.ieee.org/abstract/document/5444635/references#references

[22] E. Basalp, P. Wolf, and L. Marchal-Crespo, "Haptic Training: Which Types Facilitate (re)Learning of Which Motor Task and for Whom? Answers by a Review," *IEEE Transactions on Haptics*, vol. 14, no. 4, pp. 722–739, Oct. 2021. [Online]. Available: https://ieeexplore.ieee.org/document/9513580/

[23] J. Lee, X. Zhang, C. H. Park, and M. J. Kim, "Real-Time Teleoperation of Magnetic Force-Driven Microrobots with 3D Haptic Force Feedback for Micro-Navigation and Micro-Transportation," *IEEE Robotics and Automation Letters*, vol. 6, no. 2, pp. 1769–1776, 2021.

[24] G. Ciuti, M. Salerno, G. Lucarini, P. Valdastri, A. Arezzo, A. Menciassi, M. Morino, and P. Dario, "A comparative evaluation of control interfaces for a robotic-aided endoscopic capsule platform," *IEEE Transactions on Robotics*, vol. 28, no. 2, pp. 534–538, Apr. 2012.

[25] C. Pacchierotti, V. Magdanz, M. Medina-Sánchez, O. G. Schmidt, D. Prattichizzo, and S. Misra, "Intuitive control of self-propelled microjets with haptic feedback," *Journal of Micro-Bio Robotics*, vol. 10, no. 1-4, pp. 37–53, 2015.

[26] C. Pacchierotti, F. Ongaro, F. Van Den Brink, C. Yoon, D. Prattichizzo, D. H. Gracias, and S. Misra, "Steering and Control of Miniaturized Untethered Soft Magnetic Grippers with Haptic Assistance," *IEEE Transactions on Automation Science and Engineering*, vol. 15, no. 1, pp. 290–306, 2018.

[27] D. Powell and M. K. O'Malley, "The Task-Dependent Efficacy of Shared-Control Haptic Guidance Paradigms," *IEEE Transactions on Haptics*, vol. 5, no. 3, pp. 208–219, 2012, conference Name: IEEE Transactions on Haptics. [Online]. Available: https://ieeexplore.ieee.org/abstract/document/6257390

[28] N. Panagiotopoulos, R. L. Duschka, M. Ahlborg, G. Bringout, C. Debbeler, M. Graeser, C. Kaethner, K. Lüdtke-Buzug, H. Medimagh, J. Stelzner, T. M. Buzug, J. Barkhausen, F. M. Vogt, and J. Haegele, "Magnetic particle imaging: current developments and future directions," *International journal of nanomedicine*, vol. 10, pp. 3097–3114, 2015.

[29] A. Munawar, Y. Wang, R. Gondokaryono, and G. S. Fischer, "A Real-Time Dynamic Simulator and an Associated Front-End Representation Format for Simulating Complex Robots and Environments," in *2019 IEEE/RSJ International Conference on Intelligent Robots and Systems (IROS)*, Nov. 2019, pp. 1875–1882.

[30] "kmammou/v-hacd: Automatically exported from code.google.com/p/v-hacd." [Online]. Available: https://github.com/kmammou/v-hacd

[31] A. J. van der Molen, P. Reimer, I. A. Dekkers, G. Bongartz, M.-F. Bellin, M. Bertolotto, O. Clement, G. Heinz-Peer, F. Stacul, J. A. W. Webb, and H. S. Thomsen, "Post-contrast acute kidney injury – Part 1: Definition, clinical features, incidence, role of contrast medium and risk factors," *European Radiology*, vol. 28, no. 7, pp. 2845–2855, Jul. 2018.

[32] F. Aghazadeh, B. Zheng, M. Tavakoli, and H. Rouhani, "Motion Smoothness-Based Assessment of Surgical Expertise: The Importance of Selecting Proper Metrics," *Sensors*, vol. 23, no. 6, p. 3146, Jan. 2023, number: 6 Publisher: Multidisciplinary Digital Publishing Institute. [Online]. Available: https://www.mdpi.com/1424-8220/23/6/3146

[33] S. Estrada, C. Duran, D. Schulz, J. Bismuth, M. D. Byrne, and M. K. O'Malley, "Smoothness of surgical tool tip motion correlates to skill in endovascular tasks," *IEEE Transactions on Human-Machine Systems*, vol. 46, no. 5, pp. 647–659, Oct. 2016, conference Name: IEEE Transactions on Human-Machine Systems. [Online]. Available: https://ieeexplore.ieee.org/abstract/document/7462178

[34] S. G. Hart and L. E. Staveland, "Development of NASA-TLX (Task Load Index): Results of Empirical and Theoretical Research," *Advances in Psychology*, vol. 52, pp. 139–183, 1988.

[35] R. H. Baayen, D. J. Davidson, and D. M. Bates, "Mixed-effects modeling with crossed random effects for subjects and items," *Journal of Memory and Language*, vol. 59, no. 4, pp. 390–412, Nov. 2008. [Online]. Available: https://www.sciencedirect.com/science/article/pii/S0749596X07001398

[36] S. Machaca, E. Cao, A. Chi, G. Adrales, K. J. Kuchenbecker, and J. D. Brown, "Wrist-Squeezing Force Feedback Improves Accuracy and Speed in Robotic Surgery Training," in *2022 9th IEEE RAS/EMBS International Conference for Biomedical Robotics and Biomechatronics (BioRob)*, Aug. 2022, pp. 1–8.

[37] J. D. Brown, J. N. Fernandez, S. P. Cohen, and K. J. Kuchenbecker, "A wrist-squeezing force-feedback system for robotic surgery training," in *2017 IEEE World Haptics Conference (WHC)*, Jun. 2017, pp. 107–112.

[38] A. Abiri, Y.-Y. Juo, A. Tao, S. J. Askari, J. Pensa, J. W. Bisley, E. P. Dutson, and W. S. Grundfest, "Artificial palpation in robotic surgery using haptic feedback," *Surgical Endoscopy*, vol. 33, no. 4, pp. 1252–1259, Apr. 2019.

[39] A. Turolla, O. A. Daud Albasini, R. Oboe, M. Agostini, P. Tonin, S. Paolucci, G. Sandrini, A. Venneri, and L. Piron, "Haptic-based neurorehabilitation in poststroke patients: a feasibility prospective multicentre trial for robotics hand rehabilitation," *Computational and Mathematical Methods in Medicine*, vol. 2013, p. 895492, 2013.